Genome-Scale CRISPR/Cas9 Screening Reveals Squalene Epoxidase as a Susceptibility Factor for Cytotoxicity of Malformin A1

Yukio Koizumi,*[a] Jun Fukushima,[b] Yayoi Kobayashi,[b] Ayumi Kadowaki,[a] Miyuki Natsui,[a] Tomokazu Yamaguchi,[a] Yumiko Imai,[c] Toshihiro Sugiyama,[a] and Keiji Kuba*[a]

Malformin A1 (MA1) is a fungus-produced cyclic pentapeptide. MA1 exhibits teratogenicity to plants, fibrinolysis-enhancing activity, and cytotoxicity to mammalian cells. To clarify the cytotoxic mechanism of MA1, we screened for the genes involved in the cytotoxicity of MA1 in monocytoid U937 cells by using a CRISPR/Cas9-based genome-wide knockout library. Screening was performed by positive selection for cells that were resistant to MA1 treatment, and single guide RNAs (sgRNAs) integrated into MA1-resistant cells were analyzed by high-through-put sequencing. As a result of the evaluation of sgRNAs that were enriched in MA1-resistant cells, *SQLE*, which encodes squalene epoxidase, was identified as a candidate gene. *SQLE*-depleted U937 cells were viable in the presence of MA1, and squalene epoxidase inhibitor conferred MA1 resistance to wild-type cells. These results indicate that squalene epoxidase is implicated in the cytotoxicity of MA1. This finding represents a new insight into applications of MA1 for treating ischemic diseases.

Introduction

Malformin A1 (MA1, Figure 1 A), a cyclic pentapeptide containing an intramolecular disulfide bond, produced by the filamentous fungus *Aspergillus niger*, was originally identified as a teratogenic substance for plants.[1–4] In a project directed towards developing a new thrombolytic agent, we rediscovered MA1 in the course of screening low-molecular-weight compounds that enhance fibrinolytic activity.[5] MA1 acts on urokinase-producing monocytes and increases cellular plasmin activity.[5,6] A recent study also showed that the activation of RSK1 by way of the MAP kinase pathway leads to an increase in urokinase expression for fibrinolytic activity enhancement of MA1.[7]

[a] Dr. Y. Koizumi, A. Kadowaki, M. Natsui, Dr. T. Yamaguchi, Prof. T. Sugiyama, Prof. K. Kuba
Department of Biochemistry and Metabolic Science
Akita University Graduate School of Medicine
1-1-1 Hondo, Akita 010-8543 (Japan)
E-mail: ykoizumi@med.akita-u.ac.jp
    kuba@med.akita-u.ac.jp

[b] Prof. J. Fukushima, Y. Kobayashi
Department of Biotechnology
Faculty of Bioresource Sciences, Akita Prefectural University
241–438 Kaidobata-Nishi, Shimoshinjo-Nakano, Akita 010–0195 (Japan)

[c] Prof. Y. Imai
Laboratory of Regulation of Intractable Infectious Diseases
National Institutes of Biomedical Innovation, Health and Nutrition
7-6-8 Saito-Asagi, Ibaraki, Osaka 567-0085 (Japan)

Supporting information and the ORCID identification numbers for the authors of this article can be found under https://doi.org/10.1002/cbic.201800769.
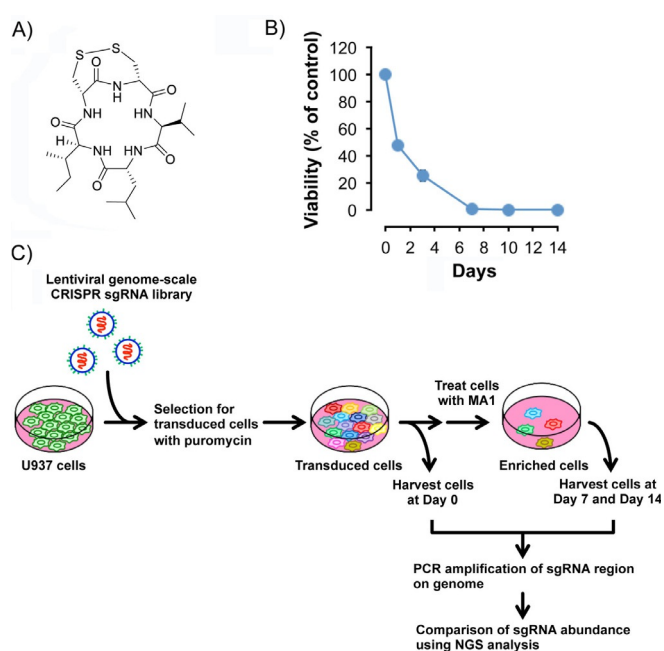
Figure 1. Schematic representation of functional screening with a CRISPR sgRNA library to search for the genes involved in the cytotoxicity of malformin A1 (MA1). A) Structure of malformin A1 (MA1). B) Cytotoxic effects of MA1 in U937 cells. U937 cells were treated with 1 μM MA1 for the periods indicated. The cytotoxicity was evaluated by 3-(4,5-dimethylthiazol-2-yl)-2,5-diphenyl-tetrazolium bromide (MTT) assay. Data are presented as means ± SDs (n = 3). C) Scheme showing MA1 resistance screen in U937 cells.

Although MA1 exhibits undesirable cytotoxicity together with the enhancement of cellular fibrinolytic activity, our previous structure–activity relationship study for MA1 suggested that the cytotoxic effects of MA1 could be split from its fibrinolysis-enhancing effect.[8] To understand the molecular structural characteristics that reduce MA1 cytotoxicity, it is important to

clarify the mechanism of action involved in the expression of cytotoxicity.

In general, elucidation of the mechanisms of action of bioactive compounds is accompanied by difficulty. Genome-wide loss-of-function screening has proven to be a powerful and unbiased approach by which to gain insight into biology modulated by bioactive compounds. Comprehensive RNA interference (RNAi) screening had been established as a searching method for gene targets and the mechanisms of action of bioactive compounds.[9–11] In recent years, genome-wide knockout screening by using the clustered regularly interspaced short palindrome repeats (CRISPR)/Cas9 genome-editing technology has been developed.[12–14] These screening approaches are extremely effective in identifying—by means of a proliferation-based assay—genes that confer a resistance or sensitive phenotype to a cytotoxic compound.[15,16]

Here, we attempted to screen the gene involved in MA1 cytotoxicity by using a genome-wide CRISPR/Cas9 knockout lentivirus library to elucidate the mechanism of MA1 cytotoxicity. As a consequence, squalene epoxidase (SQLE, EC 1.14.14.17), an important enzyme in cholesterol biosynthesis, was identified as a gene implicated in MA1 cytotoxicity.

Results and Discussion

As shown in the previous report,[8] MA1 exhibits cytotoxic properties against monocytoid U937 cells (Figure 1B). To clarify the mechanism of MA1 cytotoxicity, we therefore attempted to perform genome-wide loss-of-function screening by utilizing CRISPR/Cas9 genome editing technology. A pooled genome-scale CRISPR/Cas9 knockout (GeCKO) library, composed of a single lentiviral vector simultaneously delivering single guide RNAs (sgRNAs) and Cas9, was used for screening.[13,17] The GeCKO library consists of 123 411 sgRNAs targeting 19 052 genes in the human genome. The sgRNAs are designed to target 5' constitutive exons and to minimize off-target effects. To identify gene knockouts that result in resistance to MA1 in U937 cells, we conducted positive selection screening to select for cells acquiring MA1 resistance with lentivirus-mediated Cas9/sgRNA transduction (Figure 1C).

The concentration of MA1 used for screening (1 μM) was set as the value that would ensure cell death of nontransduced cells during 7–14 d treatment (Figure 1B). Treatment with MA1 resulted in growth arrest of GeCKO-transduced U937 cells over 14 d (Figure 2A), thus suggesting that sgRNA/Cas9-mediated modification could enrich a small group of cells resistant to MA1. When the candidate genes targeted by sgRNA that were enriched as compared to untreated control cell group were sought by next-generation sequencing after PCR amplification of the sgRNA sequence (Figure S1 and Table S1 in the Supporting Information), the sgRNA distributions of the cells after 7 and 14 days of treatment with MA1 were found to be significantly different from those of untreated control cells (one-way analysis of variance (ANOVA) with the Tukey post-hoc test, $p = 0.026$ and $p < 0.0001$, respectively, Figure 2B). Figure 2C shows the scatter plots of each sgRNA read count between MA1-treated and untreated group. Each sgRNA was ranked by its

differential abundance between the MA1-treated versus untreated populations (Figure 2D). Further, a one-sided two-sample Kolmogorov–Smirnov test was applied to calculate a p value for each gene to compare the sgRNAs targeting the gene against the nontargeting control sgRNAs (Figure 2E). Twelve overlapping sgRNAs (RAB14, SQLE, MKNK1, DEGS1, ITCH, ORMDL3, RB1CC1, C15orf32, AP3B1, ABTB2, ATG16L1, and PPP1R14A) were present between the top 100 most enriched sgRNAs at each treatment point (Figure 2F and G, and Table S2).

Of these candidate genes, SQLE, a cholesterol biosynthesis enzyme,[18,19] DEGS1, a desaturase involved in the formation of ceramide,[20] and ORMDL3, a negative regulator of sphingolipid synthesis,[21] are involved in lipid metabolism, and each gene product is localized in the endoplasmic reticulum (ER) membrane. RAB14, belonging to the large RAB family of low-molecular-mass GTPases,[22] and AP3B1, a subunit of adaptor-related protein complex 3,[23] are involved in membrane trafficking, so these candidates might participate in the intracellular transport of MA1. Moreover, two autophagy-related genes are also candidates: ATG16L1, a component of ATG12·ATG5·ATG16L1 complex involved in the autophagy process,[24] and RB1CC1, a regulator for membrane targeting of ATG16L1.[25] PPP1R14A, a regulatory subunit of protein phosphatase 1 (PP1), might also participate in autophagy as an inhibitor of PP1 involved in the inactivation of ATG16L1.[26,27] MA1 has previously been reported to induce autophagic cell death,[28] so these genes might be involved in cell death due to MA1. Furthermore, two candidate genes are involved in the ubiquitin/proteasome system: ITCH, Itchy E3 ubiquitin protein ligase,[29] and ABTB2, ankyrin repeat and BTB domain containing 2.[30] MKNK1, MAP kinase signal-integrating kinase 1, encodes a Ser/Thr kinase,[31] and C15orf32, chromosome 15 open reading frame 32, encodes an uncharacterized protein.

Our recent report showed that fluorescence-labeled MA1 was enriched in ER-like intracellular compartments,[7] so, out of the candidate genes, we focused on SQLE localized in ER membrane (Figure 2G) and validated the effects of depletion by individual sgRNA transduction on MA1 cytotoxicity in U937 cells. Protein expression levels of SQLE were depleted by about 70% or more after sgRNA transduction (Figure 3A). Whereas control sgRNA-transduced cells were dead after 10 d MA1 treatment, the deletion of SQLE provided resistance to MA1 cytotoxicity in U937 cells (Figure 3B). In addition, tolnaftate, an inhibitor of SQLE,[32] attenuated the MA1 cytotoxicity in a similar way to SQLE depletion (Figure 3C). These findings indicated that SQLE is involved in the expression of MA1 cytotoxicity.

This study demonstrated that SQLE deletion conferred resistance to MA1 cytotoxicity in U937 monocytoid cells, thus suggesting that SQLE might be a target gene of MA1. SQLE is an endoplasmic reticulum membrane enzyme involved in cholesterol biosynthesis by catalyzing the conversion of squalene into (S)-2,3-epoxysqualene.[18,19] It is as yet unknown whether MA1 acts directly on SQLE and inhibits enzyme activity. The inhibition of SQLE leads to a decrease in cholesterol biosynthesis and to the accumulation of squalene, which might result in cell death. Indeed, Sqle knockout mice are embryonic lethal,[33]
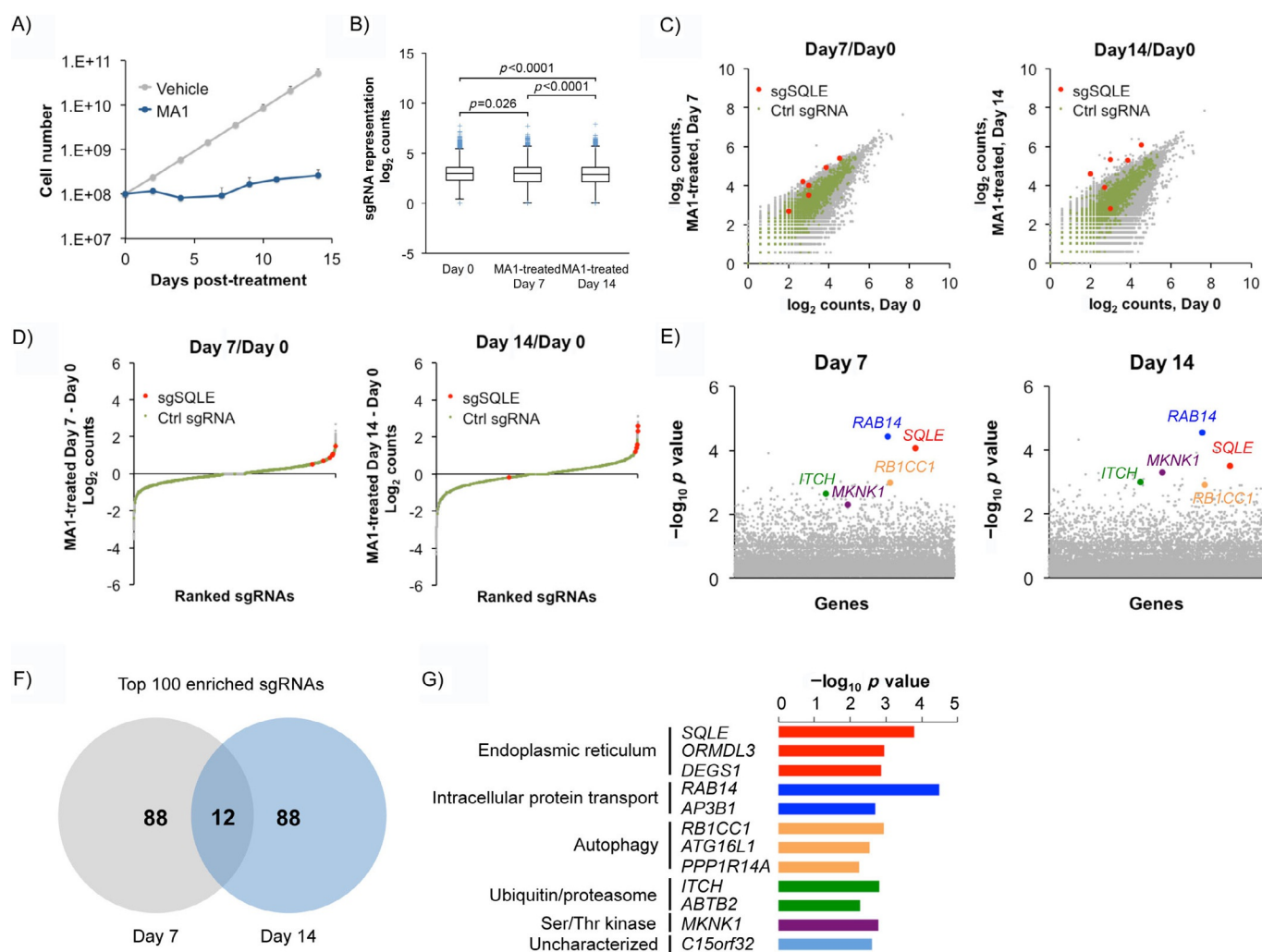
Figure 2. Lentiviral CRISPR screening to identify the gene involves in the cytotoxicity of malformin A1. A) Growth of GeCKO-transduced U937 cells. Transduced cells were treated with vehicle (DMSO) or 1 μM MA1 for 14 d. B) Box-whisker plot showing the distribution of sgRNA frequencies at each time point of MA1 treatment. The box extends from the first to the third quartile, with the whiskers denoting 1.5 times the interquartile range. Statistical analyses were performed by using one-way ANOVA with the Tukey post-hoc test. C) Scatter plots between MA1-treated and untreated populations. The enrichment of SQLE sgRNAs was observed after MA1 treatment. SQLE sgRNAs are highlighted in red. D) sgRNA ranking determined from the difference in abundance between MA1-treated and untreated populations. SQLE sgRNAs are highlighted in red. E) Gene hit identification by comparing differential abundances of all sgRNAs targeting a gene with differential abundances of nontargeting sgRNAs in a one-sided Kolmogorov–Smirnov test. F) Twelve sgRNAs overlapped between the top 100 most enriched sgRNAs 7 and 14 d after MA1 treatment. G) Gene ontology in twelve overlapped sgRNAs.

and *SQLE* is considered to be essential for development and survival. In this study, the cell proliferation of U937 cells was hardly affected by CRISPR/Cas9-induced depletion of SQLE (Figure 3B), which might possibly be compensated for by the transport of serum-derived cholesterol into the cells. Therefore, it is considered that MA1 does not inhibit the enzymatic activity of SQLE. Other genes in the cholesterol biosynthesis pathway were not found as high-ranking genes in this screening, so cholesterol biosynthesis might not be directly related to MA1 cytotoxicity (Figure S2). Rather, it is conceivable that SQLE might be a modulator of MA1 cytotoxicity. We speculate that SQLE might be involved in metabolizing MA1 into a more toxic form. This hypothesis is supported by the fact that the SQLE inhibitor counteracted the cytotoxicity of MA1 (Figure 3C). However, in view of the partial but not complete

rescue of MA1 cytotoxicity by SQLE sgRNA or TNF, we assume that other genes including *RAB14* are also involved in MA1 cytotoxicity.

We originally identified MA1 as a fibrinolysis-enhancing agent, so the cytotoxic effect is considered to be an undesirable side effect. Recent reports, however, focus on the cytotoxic effect of MA1 and its analogues, and malformins have been re-evaluated as antitumor agents.[28, 34, 35] In investigations of the mechanism of action of MA1 cytotoxicity on prostate cancer cells, oxidative stress and mitochondrial damage were reported to induce cell death.[28] In addition, MA1 has been reported to upregulate the phosphorylation of stress-activated kinase p38 followed by induction of apoptosis in colorectal cancer cells.[35] In this anticancer activity, SQLE might be associated with the cytotoxic effect of MA1.
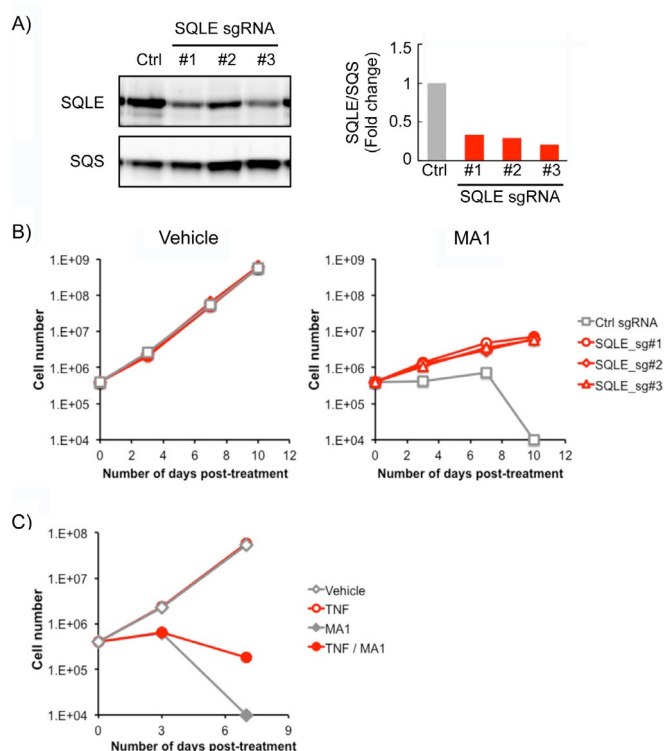
A)

B)

C)

Figure 3. SQLE is involved in the cytotoxicity of malformin A1. A) Western blot analysis of SQLE-depleted cells. Membrane fractions of sgRNA/Cas9-transduced U937 cells were applied. Squalene synthase (SQS) was used as a loading control. B) Cell viability test of SQLE-depleted cells. Control sgRNA- or SQLE sgRNA-transduced U937 cells were treated with vehicle (DMSO) or 1 μM MA1. The viable cell numbers were counted by trypan blue exclusion at the indicated time points. C) Effect of tolnaftate on MA1 cytotoxicity. U937 cells were treated with vehicle (DMSO) or with 1 μM MA1 and/or 1 μM tolnaftate (TNF). The viable cell numbers were counted by Trypan Blue exclusion at the indicated time points.

In summary, we have found, by use of genome-wide CRISPR/Cas9 screening, that SQLE is implicated in the cytotoxicity of MA1. This finding might provide new insight into applications of MA1 to treat ischemic diseases such as myocardial infarction and cerebral infarction.

Experimental Section

Reagents and cell culture: MA1 was isolated from culture broth of *A. niger* F7586 according to the previous report.[6] Briefly, *A. niger* F7586 was grown by static culture at 25 °C for 6 d. The obtained mycelial cake was extracted with methanol. The concentrated extract was re-extracted with ethyl acetate. MA1 was partially purified by silica gel column chromatography and finally purified by preparative reversed-phase HPLC. The purity of MA1 was >99%. The human GeCKOv2 CRISPR knockout pooled library was a gift from Feng Zhang (Addgene, cat# 1000000048). U937 cells (JCRB, Japan, cat# IFO50038) were cultured in RPMI-1640 containing fetal bovine serum (FBS, 10%), penicillin (100 units mL^{-1}), and streptomycin (100 μg mL^{-1}). 293FT cells were obtained from Thermo Fisher Scientific (cat# R70007) and were cultured in complete medium consisting of Dulbecco's modified Eagle's medium (DMEM), FBS (10%), L-

glutamine (6 mM), non-essential amino acids (0.1 mM), sodium pyruvate (1 mM), penicillin (100 units mL^{-1}), and streptomycin (100 μg mL^{-1}). Cells were cultured under humidified CO$_2$ (5%) at 37 °C.

MTT assay: Cytotoxicity was evaluated by means of the MTT assay. U937 cells were either passaged or replaced with fresh medium with vehicle or MA1 (1 μM) every 3–4 d. After the treatment period, MTT (Sigma–Aldrich) was added to each well, followed by incubation for 4 h. After incubation, each well received extraction solution, containing DMF (40%), CH$_3$COOH (2%), HCl (0.03 M), and SDS (20%), and was thoroughly mixed by agitation overnight at room temperature. Cytotoxicity was evaluated by measuring the absorbance at 570 nm with a microplate reader (Bio-Rad, USA).

Genome-wide loss-of-function screening

Lentivirus production: To produce lentivirus, 293FT cells were seeded in 12 100 mm dishes at ≈25% confluence the day before transfection. Prior to transfection, media were replaced with fresh media. Transfection was performed with FuGENE HD (Promega). For each dish, FuGENE HD (50 μL) was added to Opti-MEM (Thermo Fisher Scientific, 800 μL) with GeCKOv2 plasmid library (8.5 μg), pMD2.G (Addgene, cat# 12259, 4.25 μg), and psPAX2 (Addgene, cat# 12260, 4.25 μg). The mixture was incubated for 15 min before being added to cells. After 12 h, the medium was replaced with fresh medium. After 48 h, the supernatants containing viral particles were harvested and filtrated through a membrane (0.45 μm pore).

Cell transduction of the GeCKOv2 library: To transduce the GeCKOv2 library, U937 cells were seeded in ten 100 mm dishes (4× 10^6 per dish), and the cells in each dish were transduced with virus supernatant (5 mL) at a multiplicity of infection (MOI) of 0.5. After 24 h, each medium was replaced with fresh medium containing puromycin (2 μg mL^{-1}). Puromycin selection was carried out for 4 d.

MA1-resistance screen: Puromycin-selected transduced U937 cell cultures were each divided into two fractions. One fraction (3.5× 10^7 cells) was frozen down as an untreated day 0 sample for genomic DNA analysis in each case, and the other (1.4×10^8 cells) was treated with MA1 (1 μM) for 7 d. Treated cells were either passaged or replaced with fresh medium containing MA1 every 2–3 d. After 7 d, the cells were further divided into two fractions. One fraction (6.2×10^7 cells) was frozen down as a day 7 sample, and the other (2.2×10^7 cells) was treated with MA1 for an additional 7 d. After treatment, the cells (7.4×10^7 cells) were frozen down as a day 14 sample.

Genomic DNA sequencing: Frozen cell pellets were thawed, and genomic DNA was extracted from 1×10^7 cells in DNA extraction buffer containing Tris·HCl (pH 9.0, 50 mM), EDTA (20 mM), NaCl (40 mM), SDS (1%), and proteinase K (0.5 mg mL^{-1}) at 55 °C overnight. The extracted DNA was precipitated with isopropanol and washed with ethanol (70%). For next-generation sequencing (NGS) analysis, PCR was performed in two steps. For the first PCR, to amplify sgRNA integrated into genomic DNA, genomic DNA (60–70 μg per sample) was used, and 12–14 separate reaction mixtures (50 μL) with genomic DNA (5 μg in each case) were subjected to PCR with ExTaq HS polymerase (TaKaRa, Japan). The resulting amplicons were combined for a second PCR reaction. The first PCR primer sequences are: fwd: 5′-AATGG ACTAT CATAT GCTTA CCGTA ACTTG AAAGT ATTTC G-3′, rev: 5′-TCTAC TATTC TTTCC CCTGC ACTGT TGTGG GCGAT GTGCG CTCTG-3′. For the second PCR, to attach Illumina adaptors and barcodes, reaction mixtures (100 μL)

containing the first PCR amplicons (5 µL) were used. The second PCR primer sequences are: fwd: 5′-AATGA TACGG CGACC ACCGA GATCT ACACT CTTTC CCTAC ACGAC GCTCT TCCGA TCT (1–8 bp variable-length sequence, 8 bp barcode) TCTTG TGGAA AGGAC GAAAC ACCG-3′, rev: 5′-CAAGC AGAAG ACGGC ATACG AGATG TGACT GGAGT TCAGA CGTGT GCTCT TCCGA TCTTC TACTA TTCTT TCCCC TGCAC TGT-3′. For the second PCR fwd primer, a variable-length sequence and an 8 bp barcode were included to increase library complexity and to provide multiplicity of different biological samples, respectively. For both PCR reactions, 20 amplification cycles were performed. Second PCR amplicons were gel-extracted, quantified, mixed, and sequenced by using a HiSeq 2000 instrument (Illumina, USA).

CRISPR/Cas9-induced SQLE depletion: Oligonucleotides for SQLE sgRNA (Table S3) were annealed and cloned into lentivirus transfer vector lentiCRISPRv2 (Addgene, cat# 52961) at the restriction site of BsmBI.[17] For production of recombinant lentivirus particles, confluent 293FT cells (80%) were transfected in a 6-well plate with FuGENE HD mixture containing transfer plasmid, pMD2.G, and psPAX2. After 12 h, the medium was replaced with fresh medium. After 48 h, the supernatants containing viral particles were harvested and filtrated through a membrane (0.45 µm pore). For each viral construct, U937 cells (1×10^6) were transduced in a 6-well plate with medium containing viral supernatant (1 mL). At 48 h post-transduction, puromycin selection for obtaining SQLE-depleted cells was carried out for 4 d.

Western blot analysis: The membrane fraction of sgRNA/Cas9-transduced U937 cells was isolated by using a Subcellular Protein Fractionation Kit (Thermo Fisher Scientific, cat# 78840). After determination of protein concentration, equal amounts of protein were subjected to SDS-PAGE under reducing conditions. After electrophoresis, proteins were transferred to a nitrocellulose membrane. Membranes were blocked with skim milk (5%) and then incubated with mouse monoclonal antibodies against SQLE (Santa Cruz Biotechnology, cat# sc-271651) and SQS (Santa Cruz Biotechnology, cat# sc-271602). After washing, the membranes were incubated with HRP-conjugated anti-mouse IgG antibody (GE Healthcare, cat# NA931). Subsequently, targeted proteins were detected by using an ECL Prime system (GE Healthcare, cat# RPN2232).

Cell viability test: sgRNA/Cas9-transduced U937 cells (4×10^5 cells) were plated into 24-well plates with vehicle (DMSO), or MA1 (1 µM) and/or tolnaftate (Sigma–Aldrich, 1 µM). Treated cells were either passaged or replaced with fresh medium with vehicle or drugs every 3–4 d. At each time point, the viable cell number was counted by trypan blue exclusion.

Acknowledgements

Conflict of Interest

The authors declare no conflict of interest.

[1] R. W. Curtis, *Plant Physiol.* **1958**, *33*, 17–22.
[2] R. W. Curtis, *Science* **1958**, *128*, 661–662.
[3] N. Takahashi, R. W. Curtis, *Plant Physiol.* **1961**, *36*, 30–36.
[4] M. Bodanszky, G. L. Stahl, *Proc. Natl. Acad. Sci. USA* **1974**, *71*, 2791–2794.
[5] Y. Koizumi, K. Hasumi, *J. Antibiot.* **2002**, *55*, 78–82.
[6] Y. Koizumi, H. Fukudome, K. Hasumi, *Biol. Pharm. Bull.* **2011**, *34*, 1426–1431.
[7] Y. Koizumi, K. Nagai, L. Gao, S. Koyota, T. Yamaguchi, M. Natsui, Y. Imai, K. Hasumi, T. Sugiyama, K. Kuba, *Sci. Rep.* **2018**, *8*, 5472.
[8] Y. Koizumi, K. Nagai, K. Hasumi, K. Kuba, T. Sugiyama, *Bioorg. Med. Chem. Lett.* **2016**, *26*, 5267–5271.
[9] T. R. Brummelkamp, A. W. Fabius, J. Mullenders, M. Madiredjo, A. Velds, R. M. Kerkhoven, R. Bernards, R. L. Beijersbergen, *Nat. Chem. Biol.* **2006**, *2*, 202–206.
[10] A. W. Whitehurst, B. O. Bodemann, J. Cardenas, D. Ferguson, L. Girard, M. Peyton, J. D. Minna, C. Michnoff, W. Hao, M. G. Roth, X. J. Xie, M. A. White, *Nature* **2007**, *446*, 815–819.
[11] E. V. Sheveleva, T. H. Landowski, B. K. Samulitis, G. Bartholomeusz, G. Powis, R. T. Dorr, *Mol. Cancer Res.* **2012**, *10*, 392–400.
[12] T. Wang, J. J. Wei, D. M. Sabatini, E. S. Lander, *Science* **2014**, *343*, 80–84.
[13] O. Shalem, N. E. Sanjana, E. Hartenian, X. Shi, D. A. Scott, T. Mikkelson, D. Heckl, B. L. Ebert, D. E. Root, J. G. Doench, F. Zhang, *Science* **2014**, *343*, 84–87.
[14] H. Koike-Yusa, Y. Li, E. P. Tan, M. D. C. Velasco-Herrera, K. Yusa, *Nat. Biotechnol.* **2014**, *32*, 267–273.
[15] R. M. Deans, D. W. Morgens, A. Ökesli, S. Pillay, M. A. Horlbeck, M. Kampmann, L. A. Gilbert, A. Li, R. Mateo, M. Smith, J. S. Glenn, J. E. Carette, C. Khosla, M. C. Bassik, *Nat. Chem. Biol.* **2016**, *12*, 361–366.
[16] D. Estoppey, C. M. Lee, M. Janoschke, B. H. Lee, K. F. Wan, H. Dong, P. Mathys, I. Filipuzzi, T. Schuhmann, R. Riedl, T. Aust, O. Galuba, G. McAllister, C. Russ, M. Spiess, T. Bouwmeester, G. M. C. Bonamy, D. Hoepfner, *Cell Rep.* **2017**, *19*, 451–460.
[17] N. E. Sanjana, O. Shalem, F. Zhang, *Nat. Methods* **2014**, *11*, 783–784.
[18] B. P. Laden, Y. Tang, T. D. Porter, *Arch. Biochem. Biophys.* **2000**, *374*, 381–388.
[19] S. Gill, J. Stevenson, I. Kristiana, A. J. Brown, *Cell Metab.* **2011**, *13*, 260–273.
[20] P. Ternes, S. Franke, U. Zähringer, P. Sperling, E. Heinz, *J. Biol. Chem.* **2002**, *277*, 25512–25518.
[21] D. K. Breslow, S. R. Collins, B. Bodenmiller, R. Aebersold, K. Simons, A. Shevchenko, C. S. Ejsing, J. S. Weissman, *Nature* **2010**, *463*, 1048–1053.
[22] J. R. Junutula, A. M. De Maziére, A. A. Peden, K. E. Ervin, R. J. Advani, S. M. van Dijk, J. Klumperman, R. H. Scheller, *Mol. Biol. Cell* **2004**, *15*, 2218–2229.
[23] E. C. Dell'Angelica, C. E. Ooi, J. S. Bonifacino, *J. Biol. Chem.* **1997**, *272*, 15078–15084.
[24] N. Mizushima, A. Kuma, Y. Kobayashi, A. Yamamoto, M. Matsubae, T. Takao, T. Natsume, Y. Ohsumi, T. Yoshimori, *J. Cell Sci.* **2003**, *116*, 1679–1688.
[25] T. Nishimura, T. Kaizuka, K. Cadwell, M. H. Sahani, T. Saitoh, S. Akira, H. W. Virgin, N. Mizushima, *EMBO Rep.* **2013**, *14*, 284–291.
[26] M. Eto, *J. Biol. Chem.* **2009**, *284*, 35273–35277.
[27] H. Song, J. Pu, L. Wang, J. Wu, J. Xiao, Q. Liu, J. Chen, M. Zhang, Y. Liu, M. Ni, J. Mo, Y. Zheng, D. Wan, X. Cai, Y. Cao, W. Xiao, L. Ye, E. Tu, Z. Lin, J. Wen, X. Lu, J. He, Y. Peng, J. Su, H. Zhang, Y. Zhao, M. Lin, Z. Zhang, *Autophagy* **2015**, *11*, 1308–1325.
[28] Y. Liu, M. Wang, D. Wang, X. Li, W. Wang, H. Lou, H. Yuan, *Cancer Chemother. Pharmacol.* **2016**, *77*, 63–75.
[29] A. Marchese, C. Raiborg, F. Santini, J. H. Keen, H. Stenmark, J. L. Benovic, *Dev. Cell* **2003**, *5*, 709–722.
[30] K. Koiwai, S. Maezawa, T. Hayano, M. Iitsuka, O. Koiwai, *Genes Cells* **2008**, *13*, 593–607.
[31] R. Fukunaga, T. Hunter, *EMBO J.* **1997**, *16*, 1921–1933.
[32] N. S. Ryder, I. Frank, M. C. Dupont, *Antimicrob. Agents Chemother.* **1986**, *29*, 858–860.

[33] The Jackson Laboratory, Mouse Genome Informatics Web Site, http://www.informatics.jax.org/marker/MGI:109296, **2018**.

[34] J. Wang, Z. Jiang, W. Lam, E. A. Gullen, Z. Yu, Y. Wei, L. Wang, C. Zeiss, A. Beck, E. C. Cheng, C. Wu, Y. C. Cheng, Y. Zhang, *PLoS One* **2015**, *10*, e0140069.

[35] S. Y. Park, H. H. Oh, Y. L. Park, H. M. Yu, D. S. Myung, S. B. Cho, W. S. Lee, D. Park, Y. E. Joo, *Int. J. Oncol.* **2017**, *51*, 959–966.

www.chembiochem.org
1568